

Magnetic properties of BaFe_2As_2 from spin-spiral calculations

A.N. Yaresko, G.-Q. Liu, V.N. Antonov and O.K. Andersen

The discovery of superconductivity in F-doped $\text{LaFeAsO}_{1-x}\text{F}_x$ ($T_c = 27$ K) by Kamihara and co-workers [1] initiated an avalanche of experimental and theoretical works on iron pnictides. The interest in these compounds heated up even more when superconductivity below $T_c = 38$ K was reported in completely oxygen free $\text{Ba}_{1-2y}\text{K}_{2y}\text{Fe}_2\text{As}_2$ doped with potassium, for which good quality single crystals were synthesized. Both families of the iron pnictides have a quasi 2D tetragonal crystal structure, in which FeAs layers are separated by either LaO or Ba layers. Fe ions form a square lattice sandwiched between two As sheets shifted so that each Fe is surrounded by a distorted As tetrahedron. Both stoichiometric parent compounds undergo a structural transition, at which the symmetry of the lattice lowers to orthorhombic. At the same (BaFe_2As_2) or slightly lower (LaFeAsO) temperature the so-called stripe AFM order sets in, with Fe magnetic moments ordered ferromagnetically (FM) along the shorter b -axis and antiferromagnetically (AFM) along the a - and c -axes. Electron doping of the FeAs layers in $\text{LaFeAsO}_{1-x}\text{F}_x$ suppresses the structural and magnetic transitions in favor of superconductivity already at $x = 0.03$ [2]. In $\text{Ba}_{1-2y}\text{K}_{2y}\text{Fe}_2\text{As}_2$, the transition is also suppressed but at much higher level ($2y \approx 0.3$) of K doping [3], which corresponds to the doping of the FeAs layers with 0.15 holes per Fe ion. Since the superconducting transition occurs already at $y \approx 0.1$, the superconducting and magnetically ordered phases seem to coexist in a wide range of K contents.

Although it is not clear yet whether superconductivity in the iron pnictides is mediated by AFM fluctuations or superconductivity and magnetism compete, it is difficult to overestimate the importance of understanding the magnetic properties of these compounds.

In this work the magnetic interactions between Fe moments are studied by performing self-consistent calculations for co-planar spin-spiral structures in $\text{Ba}_{1-2y}\text{K}_{2y}\text{Fe}_2\text{As}_2$ with $y = 0, 0.1, 0.2, 0.3$. The calculations were carried out

within the local-spin-density approximation on the base of the generalized Bloch theorem using the linear muffin-tin orbital method. For all doping levels the experimental room temperature crystal structure of BaFe_2As_2 was used. The effect of doping was simulated by using the virtual crystal approximation.

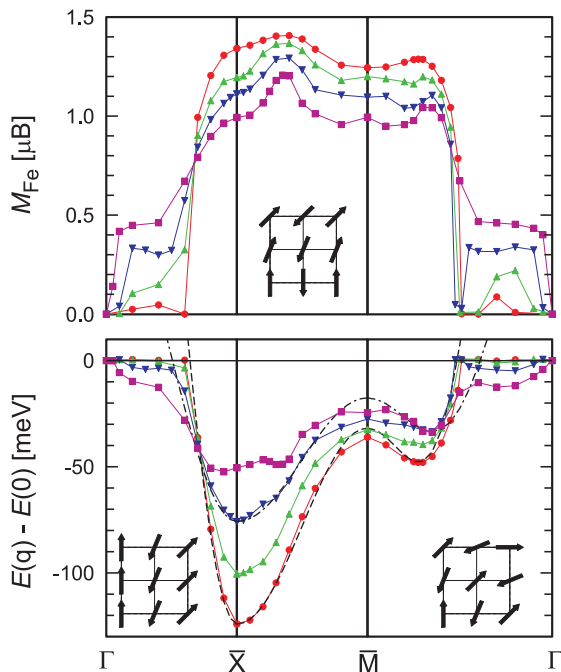


Figure 1: The dependencies of the total energy (lower panel) and Fe magnetic moment (upper panel) on the \mathbf{q} -vector of a spin spiral calculated for $\text{Ba}_{1-2y}\text{K}_{2y}\text{Fe}_2\text{As}_2$ with $y = 0$ (red), 0.1 (green), 0.2 (blue), and 0.3 (magenta). The energy of the $j_1 - j_2$ Heisenberg model for $y = 0$ and $y = 0.2$ are plotted by dashed and dash-dotted lines, respectively. The inserts show representative real-space spin-spiral structures for each direction.

The total energies were calculated for the wavevector \mathbf{q} of a spin spiral varying along the edges of the irreducible triangle of the 2D Brillouin zone (BZ) formed by Γ -, \bar{X} -, and \bar{M} -points, which in the π/d units have the coordinates $(0,0)$, $(1,0)$, and $(1,1)$, with d being the nearest Fe-Fe distance. The spin spirals with $\mathbf{q} = (1,0)$ (\bar{X}) and $(1,1)$ (\bar{M}) correspond to the stripe and checkerboard AFM orders, respectively. The total energy and Fe magnetic moment are plotted as functions of \mathbf{q} in Fig. 1. In

agreement with the experimental data the total energy minimum for the undoped BaFe_2As_2 is found at the \bar{X} -point, e.g., for the stripe AFM order. Additionally, a local minimum of $E(\mathbf{q})$ appears at $\mathbf{q}_{\min} = (0.75, 0.75)$ along the \bar{M} - Γ line. The calculated Fe magnetic moment varies weakly along the \bar{X} - \bar{M} line (Fig. 1) but rapidly decreases to zero as \mathbf{q} approaches the Γ -point.

In the range of \mathbf{q} , for which a magnetic solution exists, the calculated $E(\mathbf{q})$ curve can be surprisingly well approximated by the classical Heisenberg model on the square lattice with AFM nearest neighbor j_1 and next-nearest neighbor $j_2 > j_1/2$ interactions. The position of the local minimum at \mathbf{q}_{\min} determines the j_2/j_1 ratio of 0.77. Then, $j_1 = 95$ meV and $j_2 = 73$ meV can be estimated from the energy difference $E(\mathbf{q}_{\min}) - E(\bar{X})$, using the value of the Fe spin $S = 0.67$ calculated at the \bar{X} -point. These values of j_1 and j_2 are comparable to the values calculated for the undoped LaFeAsO [4]. The energy of the $j_1 - j_2$ Heisenberg model is compared to the calculated total energy in Fig. 1.

The hole doping of the FeAs layer due to K substitution results in strong reduction of the stabilization energy of the magnetic solution. The Fe moment calculated for the stripe AFM order decreases from $1.34\mu_B$ in the undoped compound to $0.99\mu_B$ for $y = 0.3$. Nevertheless, the stripe AFM order remains stable in a wide doping range. Only at $y = 0.3$ the total energy minimum finally shifts away from the \bar{X} -point. The calculations show that the stripe AFM order in $\text{Ba}_{1-2y}\text{K}_{2y}\text{Fe}_2\text{As}_2$ is more resistant to doping as compared to $\text{LaFeAsO}_{1-x}\text{F}_x$, in which the minimum shifts to incommensurate \mathbf{q} at much smaller level of F doping [4]. This conclusion is supported by experimental observations of the traces of the spin density wave phase at K concentration as high as 40%, i.e., well into the superconducting region.

The effective exchange coupling constants estimated for different levels of K doping are summarized in Tab. 1. The strong doping dependence of j_1 and j_2 indicates that the magnetic properties of $\text{Ba}_{1-2y}\text{K}_{2y}\text{Fe}_2\text{As}_2$ cannot be adequately described by the simple $j_1 - j_2$ Heisenberg model.

Table 1: Doping dependence of the exchange coupling constants j_1 and j_2 in $\text{Ba}_{1-2y}\text{K}_{2y}\text{Fe}_2\text{As}_2$.

y	j_1 [meV]	j_2 [meV]	j_2/j_1
0	95.0	73.1	0.77
0.1	76.7	65.2	0.85
0.2	39.1	43.1	1.10
0.3	19.4	21.3	1.10

The strength of the interlayer exchange coupling in BaFe_2As_2 was evaluated by adding a nonzero q_z component to the wavevector of the spin spiral at the \bar{X} -point. As q_z increases, the relative orientation of the Fe moments in adjacent FeAs layers changes from ferro- to antiferromagnetic one, whereas the stripe AFM order within each layer is not affected. The calculated q_z dependence of the total energy indicates that the AFM interlayer coupling in BaFe_2As_2 is significantly stronger than in LaFeAsO , in which the magnetic interactions are much more 2D-like [4].

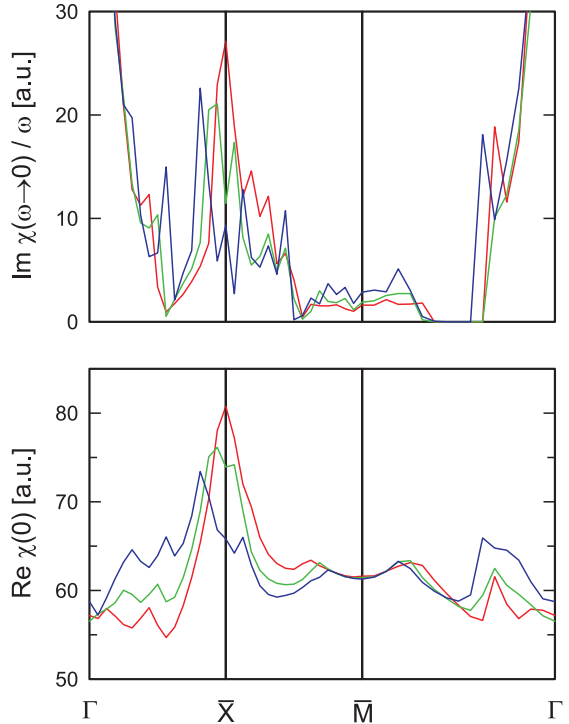


Figure 2: The real (lower panel) and imaginary (upper panel) parts of the bare susceptibility calculated for $\text{Ba}_{1-2y}\text{K}_{2y}\text{Fe}_2\text{As}_2$ with $y = 0$ (red), 0.1 (green), and 0.2 (blue).

The limit of a weak magnetic perturbation was analyzed by performing calculations of the bare transverse spin susceptibility $\chi_0(\mathbf{q}, \omega)$. Both the imaginary $\text{Im}\chi_0(\mathbf{q}, \omega \rightarrow 0)/\omega$ and real $\text{Re}\chi_0(\mathbf{q}, 0)$ parts of the susceptibility of undoped BaFe_2As_2 show sharp peaks at $\mathbf{q}=(1,0)$ (Fig. 2), which appear as a result of the nesting of quasi-two-dimensional Fermi surface (FS) sheets. Indeed, as shown in Fig. 3 corrugated hole-like cylinders around Γ match elliptical electron-like sheets centered at the \bar{X} -point, when shifted by the vector $(\pi/a, \pi/a, 0)$ which corresponds to $\mathbf{q}=(1,0)$ in the 2D BZ.

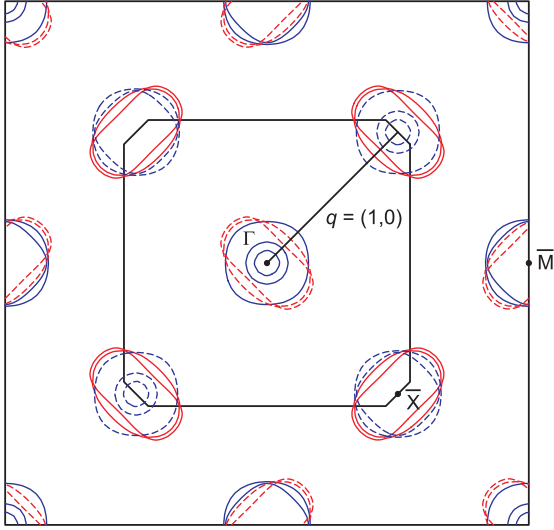


Figure 3: Fermi surface cross-sections calculated for undoped BaFe_2As_2 . Electron and hole sheets are plotted by red and blue lines, respectively. FS sheets shifted by the vector $\mathbf{q}=(1,0)$ are shown by dashed lines. The BZ boundary is plotted by solid black lines.

With the increase of K content the FeAs layer is doped with holes. As a result the hole-like cylinders around Γ expand, whereas the electron-like

sheets around \bar{X} shrink. They are no longer connected by the nesting vector $\mathbf{q}=(1,0)$ and the susceptibility at the \bar{X} -point decreases rapidly with doping. Instead, a peak develops in both the imaginary and real parts of $\chi_0(\mathbf{q}, 0)$ at those wavevectors, at which the electron- and hole-like cylinders cross each other.

In conclusion, the self-consistent total energy calculations performed for spin spirals in $\text{Ba}_{1-2y}\text{K}_{2y}\text{Fe}_2\text{As}_2$ confirm that in the undoped compounds the minimum of the total energy is reached at the wavevector $\mathbf{q}=(1,0)$, which corresponds to the stripe AFM order. The energy gain due to the formation of the magnetically ordered solution decreases with K doping, but the minimum stays at the \bar{X} -point in a wide range of K concentrations. The nesting of the hole- and electron-like FS sheets centered at the Γ and \bar{X} -points, respectively, causes the appearance of sharp peaks at $\mathbf{q}=(1,0)$ in both the imaginary and real parts of the non-interacting susceptibility of undoped BaFe_2As_2 . When the FeAs layer is doped with holes the nesting is destroyed. As a consequence, the susceptibility at $\mathbf{q}=(1,0)$ is strongly suppressed and its peak shifts to incommensurate wavevectors.

-
- [1] Kamihara, Y., T. Watanabe, M. Hirano and H. Hosono. *Journal of the American Chemical Society* **130**, 3296–3297 (2008).
 - [2] Dong, J., H.J. Zhang, G. Xu, Z. Li, G. Li, W.Z. Hu, D. Wu, G.F. Chen, X. Dai, J.L. Luo, Z. Fang and N.L. Wang. *Europhysics Letters* **83**, 27006 (2008).
 - [3] Rotter, M., M. Tegel and D. Johrendt. *Physical Review Letters* **101**, 107006 (2008).
 - [4] Yaresko, A.N., G.-Q. Liu, V.N. Antonov and O.K. Andersen. arXiv:0810.4469 (to be published in *Physical Review B*).